Available online at www.springerlink.com

Acta Metall. Sin. (Engl. Lett.) Vol.26 No.2 pp. 137—142 April 2013

ACTA
METALLURGICA SINICA
(ENGLISH LETTERS)

Elastoplastic Properties of Solid Oxide Fuel Cell Before and After Reduction

Xiang ZHAO† *and Fenghui WANG*

Department of Engineering Mechanics, Northwestern Polytechnical University, Xi'an 710129, China

[Manuscript received 12 September 2012, in revised form 21 December 2012]

Oliver Pharr method may overestimate the hardness because of the effect of pile up. In this paper, the mechanical properties of oxide fuel cell, such as hardness and elastic modulus, are determined by a work of indentation, then a reverse analysis algorithms is followed to analyze the yield strength. From the nanoindentation tests carried out for the half-cell structure of solid oxide fuel cells (SOFCs), the typical mechanical properties are derived by the work of indentation and the reverse analysis algorithms. Due to the differences of Young's modulus and the mismatch of thermal expansion coefficients in the half-cell structure (NiO-YSZ/YSZ), the residual stress, which has effects on the fuel cell's performance, is aroused during sintering. Numerical results show that the load-displacement curve is agreement with the experimental curve if the residual stress was considered.

KEY WORDS: Solid oxide fuel cell; Residual stress; Nanoindentation; Yield strength; Reduction

1. Introduction

Solid oxide fuel cells have attracted special interests as a method of future electric power generation because of high efficiency and pollution-free operation. Yet their widespread use is hindered by high costs and poor long-term thermomechanical reliability due to the different thermal expansion coefficients and particular work environments[1]. Thermal stresses can cause cracking within the microstructure or even delamination and other catastrophic failure[2]. Measuring the mechanical properties, such as elastic modulus and yield strength, is always the first critical step to analyze their mechanical integrity. However, this is often considered difficult since the conventional techniques, such as the tensile, the three-point or four point bending technique, require extensive machining efforts [3].

Several methods exist for measuring the elastic modulus and hardness of materials on the submicron scale[1]. Among them the instrumented indentation techniques (Oliver Pharr method) has become a primary technique for determining the mechanical properties of thin films and small structural features[4]. During the past decade, several important changes have been made to the method that both improve its accuracy and extend its realm of application[5]. These changes have been developed both through experience in testing a large number of materials and by improvements of testing equipment and techniques. For example, an improved methods for calibrating indenter area functions and load frame compliances[5]. However, if $h_{\rm f}/h_{\rm m}$ (final indentation depth/peak load indentation depth)>0.7, the method overestimates the hardness by as much as 100% because of the effect of pile up. In addition, all magnitude and type of internal stress have an effect on determining the elastic modulus and hardness[6,7]. For instance, the CN_x film with compressive internal stress has larger hardness and modulus than that without compressive internal stress[6].

Alternatively, because of the use of the energy dissipated or work done during the indentation, work of indentation methods can particularly be an attractive approach when a pile up effect is observed[1,8−12]. Based on the relationship among the total, plastic and elastic energy constants, a reformative work of indentation has been used to determine the hardness and

† Corresponding author. Ph.D.; Tel: +86 29 88491019; E-mail address: hope_888@mail.nwpu.edu.cn (Xiang ZHAO)

DOI: 10.1007/s40195-012-0157-6

elastic modulus of SOFC[1]. The hardness obtained by the work of indentation exhibits well agreement with the values determined by Oliver Pharr method.

Study on the determining the elastic and hardness by indentation is active, while there are few literatures focused on the study of yield strength[3]. From the principle of dimensional analysis, the relationships between the indentation load-displacement curve and material yield strength have been established by the finite element method[3]. This method can be used to elastic-perfectly plastic material and material with work hardening. However, this method is not considered the effect of residual stress.

In our previous work[13], based on Oliver-Pharr method, we have introduced the residual stress into the reverse analysis algorithms to determine the elastoplastic properties of SOFC before reduction. In this study, the work of indentation is used to determine the elastic modulus of SOFC before and after reduction, then the yield strength is obtained by the reverse analysis algorithms considering the residual stress. FE simulation is performed to verify the experiment results.

2. Analysis of Nanoindentation Data

2.1 Reverse analysis algorithms without residual stress

Useful elastic and/or plastic properties of the film material can be readily obtained from the indentation P-h loading curve by one indentation test, once the substrate modulus is known. From the numerical forward analysis, the relationships between the material properties and the indentation parameters were established based on extensive finite element simulations by Zhao *et al.*[3,14] Based on these relationships, the film material properties can be determined from the reverse analysis by performing an indentation test on the sample material, and measuring data at two different indentation depths of $t/3$ and $2t/3$ (t is the film thickness). The technique is applicable to ceramic or high-strength metal thin films whose indentation behaviors can be effective described by the phenomenological elastic-perfectly plastic material model as long as significant cracking does not occur.

From extensive finite element analyses by varying the material properties in a large range, the following functional forms can be established to relate the normalized indentation load with film/substrate properties:

$$\frac{P_1}{\sigma_{\mathrm{y}} h_1^2} = F_1\Big(\frac{E}{E_{\mathrm{s}}}, \frac{E}{\sigma_{\mathrm{y}}}\Big) \tag{1a}$$

$$\frac{P_2}{\sigma_{\mathrm{y}} h_2^2} = F_2\Big(\frac{E}{E_{\mathrm{s}}}, \frac{E}{\sigma_{\mathrm{y}}}\Big) \tag{1b}$$

where $h_1 = t/3$ and $h_2 = 2h/3$; E and σ_{y} are Young's modulus and yield stress of film respectively; E_{s} is the modulus of substrate. The functions can be fitted in the following form[3]:

$$\ln\Big(\frac{P_1}{\sigma_{\mathrm{y}} h_1^2}\Big) = (P_1 + P_2\xi + P_3\xi^2 + P_4\eta + P_5\eta^2 + P_6\eta^3)/ (1 + P_7\xi + P_8\eta + P_9\eta^2) \tag{2a}$$

$$\ln\Big(\frac{P_2}{\sigma_{\mathrm{y}} h_2^2}\Big) = (P_1 + P_2\xi + P_3\xi^2 + P_4\eta + P_5\eta^2 + P_6\eta^3)/ (1 + P_7\xi + P_8\eta + P_9\eta^2) \tag{2b}$$

here, ξ=ln(E/E_{s}) and η=ln(E/σ_{y}). These two functions relate the indentation response with the film elastoplastic properties as well as film/substrate elastic mismatch. They can be employed in the reverse analysis for determining the film properties[3].

2.2 Reverse analysis algorithms with residual stress

Without consideration the residual stress, the relation between the mechanical properties of the film and the $P-h$ load curve was given by Eq. (1). However, residual stress is an inevitable universal phenomenon when co-firing or preparation. Depending on the deposition process and the deposition parameters, these stresses can be either compressive or tensile.

If we get the residual stress σ_{r} of the film, Eq. (1) can be rewritten as

$$\frac{P_1}{(\sigma_{\mathrm{y}} + \sigma_{\mathrm{r}}) h_1^2} = F_1\Big(\frac{E}{E_{\mathrm{s}}}, \frac{E}{(\sigma_{\mathrm{y}} + \sigma_{\mathrm{r}})}\Big) \tag{3a}$$

$$\frac{P_2}{(\sigma_{\mathrm{y}} + \sigma_{\mathrm{r}}) h_2^2} = F_2\Big(\frac{E}{E_{\mathrm{s}}}, \frac{E}{(\sigma_{\mathrm{y}} + \sigma_{\mathrm{r}})}\Big) \tag{3b}$$

Residual stress, in the film, can be calculated analytically according to the thermal misfit theory, the residual expressed by[13,15]

$$\sigma_{\mathrm{r}} = E\Delta\alpha\Delta T/(1-\nu) \tag{4}$$

where $\Delta\alpha$=$\alpha_2 - \alpha_1$, α_2 and α_1 denote thermal expansion coefficient of substrate and film, respectively; ΔT denotes temperature difference from sintering to room temperature; ν denotes Poisson ratio.

2.3 Elastic modulus of substrate

In nanoindentation, Young's modulus of substrate could be calculated by the load-displacement curves through the Oliver-Pharr method. However, if $h_{\mathrm{f}}/h_{\mathrm{m}} > 0.7$, the Oliver-Pharr method may overestimate the hardness by as much as 100% because of the effect of pile up. Alternatively, the hardness H can be calculated using the work of indentation:

$$H = \frac{\kappa W(n+1)}{h_{\mathrm{m}} h_{\mathrm{c}}^2} = \kappa\frac{P_{\mathrm{m}}}{h_{\mathrm{c}}^2} \tag{5}$$

where the relationship between contact depth and maximum displacement is given by Attaf [11]:

$$h_{\mathrm{c}} = \frac{2(\gamma_{\mathrm{E}} - 1)}{(2\gamma_{\mathrm{E}} - 1)} h_{\mathrm{m}} \tag{6}$$

where γ_E is the elastic energy constants, defined as

$$W_S = \gamma_E W_E \tag{7}$$

Once we know the hardness by the work of indentation approach Eq. (5), elastic modulus can be determined by following equation [5]:

$$\frac{W_T - W_E}{W_T} \cong 1 - 5\frac{H}{E_r} \tag{8}$$

where E_r is the reduced modulus, which combines modulus of both the indenter and specimen. Considering the properties of the diamond indenter, the reduced modulus could have the following relationship:

$$\frac{1}{E_r} = \frac{(1-\nu_s^2)}{E_s} - \frac{(1-\nu_i^2)}{E_i} \tag{9}$$

If we substituted Eq. (8) into Eq. (9), the E and σ_y of film can be calculated using Eq. (1) or Eq. (3).

3. Experimental Procedure

The half-cell structure of SOFC was made by Ningbo Institute of Material Technology and Engineering, Chinese Academy of Sciences (Ningbo, China). The anode-supported cells were fabricated by co-firing the thin electrolyte (YSZ) on the anode substrate (NiO-YSZ) at 1400 °C. The thickness of YSZ film and NiO-YSZ substrate were about 10 μm and 310 μm, respectively. For measuring the anode mechanical properties after reduction, NiO-YSZ/YSZ composite ceramic was reduced in H_2-4%N_2 at 800 °C to make Ni-YSZ/YSZ cermets.

Before indentation testing using Berkovich diamond in MTS Nano Indenter II, each specimen with dimension of 0.32 mm (height)×11 mm (width)× 15 mm (length) was sandwiched in middle between epoxy. The system has load and displacement resolutions of 1 mN and 0.04 nm. Fig. 1 shows the cross-section of the test sample which polished before test. The indentation points are perpendicular to the half-cell structure interface of SOFC. Among six points, four points are on film side and two on anode side, respectively. The indenter was first loaded to the peak load 20 mN which was held constant for 10 s, then unloading terminated at 10% of the peak load with another 100 s holding period to allow any final time dependent plastic effects to diminish, and the specimen was fully unloaded. According to our early published study[1], the indentation point A1 which is far from the interface was held to avoid the substrate effect in hardness testing, and the film can be considered as bulk material due to the shallow indentation depth.

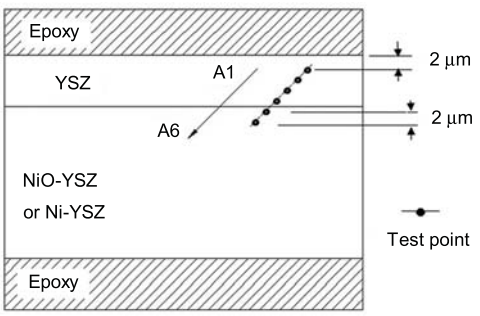

Fig. 1 Schematic of testing sample and indentation points of the experiments

4. Results and Discussion

4.1 Elastic modulus and hardness of SOFC

Fig. 2 presents the experimental data of NiO-YSZ/YSZ and Ni-YSZ/YSZ for indentations made to peak load of 20 mN. The differences in hardness are apparent from the large differences in the depth. The hardest is YSZ film, and the softest region is in substrate. The whole results in terms of load, displacements and elastic modulus (by Eq. (8)) are presented in Table 1.

4.2 Yield strength of SOFC without residual stress

The maximum indentation depth is not more than 500 nm, the thickness of YSZ film is 10 μm. Due to the depth of A1which far from the anode substrate (about 8 μm) is 242.5 nm, the effect of anode substrate on the mechanical properties of YSZ film is little. The film could be think as a bulk material during the nanoindentation test, the yield strength of film can be calculated by Eq. (1). Different is, the further

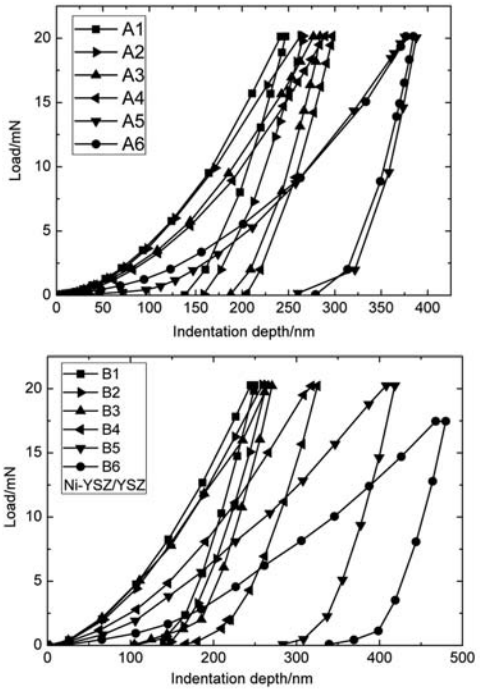

Fig. 2 Experimental indentation force-displacement curves

the indentation points is from the interface, the greater is the hardness and modulus of film.

Corresponding to $2t/3$ and $t/3$, the indentation load are 20.14 mN and 5.54 mN when the test indentation depth are 242.5 nm and 121.3 nm, respectively. The elastic modulus of A1 calculated by the work of indentation is 224.46 GPa, the yield strength of A1 calculated by Eq. (1) is 6.21 GPa. Because test point A1 is far from the interface, the yield strength values of YSZ can be considered as 6.21 GPa, without considering the residual stress.

Similarly, Table 1 compares the yield strength of each test point in two material systems. Because test points A1 (or B1) and A6 (or B6) are all far from the interface, the yield strength values of YSZ, NiO-YSZ and Ni-YSZ can be considered as 6.21 GPa, 2.56 GPa and 1.23 GPa, respectively. It can be seen that the yield strength of substrate is decreased by 52% due to NiO-YSZ reduced to Ni-YSZ. In addition, as shown in Table 2, the elastic modulus and hardness of substrate are decreased by 34% and 48%, respectively.

4.3 Yield strength of SOFC with residual stress

The anode-supported cells are fabricated by co-firing the thin electrolyte on the anode substrate at 1400 °C, then cooling to home temperature. The thermal expansion coefficients (TEC) of YSZ, NiO-YSZ and Ni-YSZ are $10.8\times10^{-6}/°C$, $13\times10^{-6}/°C$ and $12.5\times10^{-6}/°C$[15,16], respectively. The residual stress in YSZ film is then calculated by Eq. (4). However, the reduction procedure causes a drastic modification of the microstructure, which cannot be modelled by Eq. (4), the thermal expansion coefficient will change from $13\times10^{-6}/°C$ into $12.5\times10^{-6}/°C$ at 800 °C. Due to the bending theory, the residual stress in substrate layer is [15]:

$$\sigma_{r2} = E_s(\varepsilon - \alpha_2 \Delta T) \tag{14}$$

where ε is linear bending strain caused by residual stress. As shown in Fig. 3, substituting $\sigma_{r2}=-901$ MPa into Eq. (3), the yield strength of A1 is calculated and listed in Table 1.

Similarly, the yield strength with residual stress of each test point in two material systems is shown in Table 1. When the residual stress was considered, the yield strength values of YSZ, NiO-YSZ and Ni-YSZ is 7.11 GPa, 2.53 GPa, 1.20 GPa, respectively. It can be seen that the yield strength values computed by Eq. (3) are higher than Eq. (1), as shown in Table 1. According to empirical formula[17], the ratio between the hardness and yield strength, λ, is 2.5–3.0. The ratios λ_1, λ_2 (without and with residual stress) are listed in Table 1 for both two material systems. The ratio λ_1 for test point A1 is higher than empirical formula, if the residual stress is not taken into account. On the contrary, λ_2 is in agreement with the empirical formula. However, in the region of interface, these ratios should be further researched because of the complicated stress field and the location uncertainty in test points A5 and B6.

Table 1 Mechanical properties of the indentation region

Sample	Test point	E/GPa	H/GPa	σ_y/GPa(Eq. (1))	σ_y/GPa(Eq. (3))	λ_1	λ_2
NiO-YSZ/YSZ	A1	224.46	21.30	6.21	7.11	3.43	3.00
	A2	209.36	17.73	5.63	6.53	3.15	2.72
	A3	197.92	13.78	3.82	4.72	3.61	2.92
	A4	179.36	12.70	3.67	4.57	3.46	2.78
	A5	129.65	6.64	2.11	2.08	3.15	3.19
	A6	130.68	7.07	2.56	2.53	2.76	2.79
Ni-YSZ/YSZ	B1	227.28	21.39	6.42	7.09	3.38	3.02
	B2	205.77	19.04	6.19	6.86	3.07	2.78
	B3	204.26	17.37	5.99	6.66	2.90	2.61
	B4	176.07	10.73	3.57	4.24	3.01	2.53
	B5	117.02	5.92	2.61	2.58	2.26	2.29
	B6	85.68	3.68	1.23	1.20	2.99	3.06

Table 2 Mechanical properties of two material systems

Material	E/GPa	H/GPa	σ_y/GPa(Eq. (1))	σ_y/GPa(Eq. (3))
YSZ	224.46	21.30	6.21	7.11
NiO-YSZ	130.68	7.07	2.56	2.53
Ni-YSZ	85.68	3.68	1.23	1.20

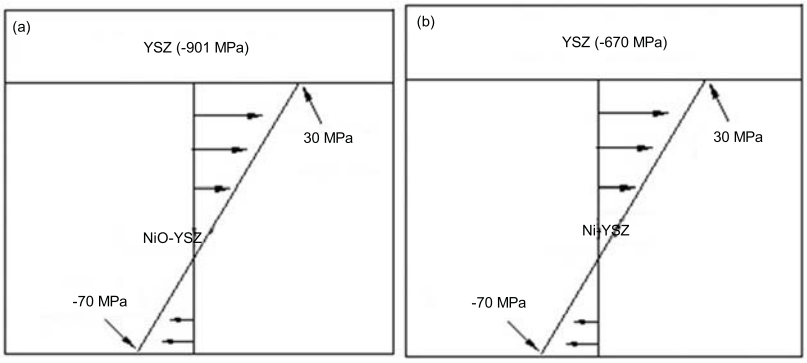

Fig. 3 Residual stress distribution in film/substrate system: (a) NiO-YSZ/YSZ; (b) Ni-YSZ/YSZ

5. Numerical Results

In the present work, we have studied the nanoindentation process of YSZ film on NiO-YSZ (and Ni-YSZ) substrate. In addition, we have verified if this process is appropriate by performing an analysis with a three-dimensional model. Due to the complexity of the phenomena involved in the indentation process, we used the FE program ABAQUS which allows effective modeling of non-linear problems such as the materials properties, the contact between two bodies and the large deformations of the material under the indenter.

Nanoindentation by a three-sided Berkovich indenter with an included half-angle, 65.3, was simulated. The film/substrate materials were represented by reduced integration elements (C3D8R element type[18]). It is known that the region of interest, which is in the vicinity of the indenter tip, is very small compared with the overall specimen size. Accurate FE simulations require fine mesh in the region of interest. The friction coefficient between the indenter tip and cross-section of the specimen surface is assumed to be zero[18], as shown in Fig. 4. The interface of thin films and substrates is defined as perfectly bonded. Both the film and the substrate are assumed to be homogeneous and isotropic and having a perfect elastic-plastic behavior.

According to the experiment A1, the nanoindentations have been performed on NiO-YSZ/YSZ system with different situations: the initial thermal stress field is considered or not. The elastic modulus and Poisson's ratio of YSZ are set to be 224.46 GPa and 0.3. The same parameters are 130.68 GPa and 0.3 for NiO-YSZ and 1141 GPa and 0.25 for the indenter.

In the first simulation, the residual stress is neglected in the finite element simulations. The yield strength of YSZ is set to be 6.21 GPa. In the second, the thermal residual stress field shown in Fig. 5 is taken as the initial stress field to simulate the load-displacement curve under nanoindentation. The yield strength of YSZ is set to be 7.11 GPa. Fig.6 shows that the load-displacement curve is agreement with the experiment curve if the residual stress was considered.

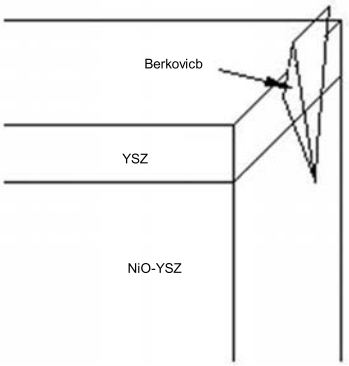

Fig. 4 3D FEM model of SOFC

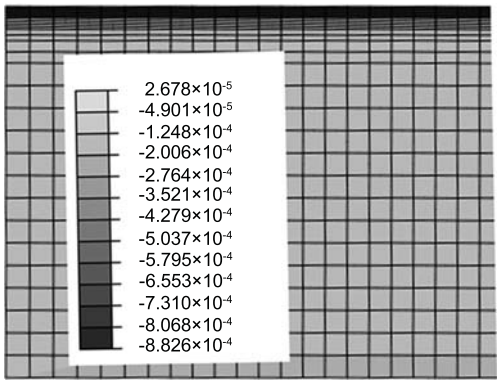

Fig. 5 Thermal residual stress field: multiply the values in legend by 10^6

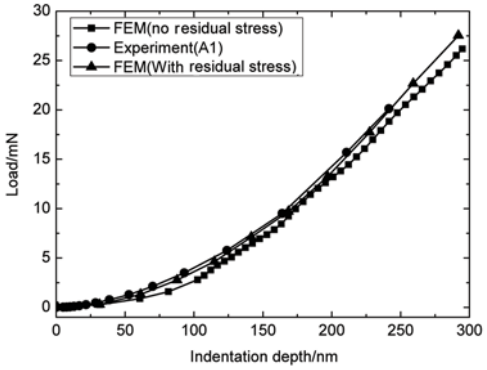

Fig. 6 Comparison of experimental indentation force-displacement curves and numerical results considered residual stress or not

6. Conclusions

The mechanical properties such as elastic modulus, coefficient of thermal expansion and yield strength of SOFC will change before and after reduction. Nanoindentation tests were carried out for the half cell structure of SOFCs before and after reduction.

Using the work of indentation, the elastic modulus and hardness of SOFC is determined. And then the yield strength is determined by the reverse analysis algorithms with residual stress. Results show that, the hardness, elastic modulus and yield strength of YSZ film are higher than that of substrate NiO-YSZ or Ni-YSZ. With reducing to Ni-YSZ, hardness, elastic modulus and yield strength of substrate can be decreased by almost 50%. A three-dimensional model was used to verify the nanoindentation process. It is found that the load-displacement curve is agreement with the experiment curve if the residual stress was considered.

Acknowledgements

This work was supported by the National Natural Science Foundation of China (No. 10772146) and Excellent Doctorate Foundation of Northwestern Polytechnical University.

REFERENCES

[1] X. Zhao, F. Wang, J. Hang and T. Liu, J. Power. Sources **201** (2012) 231.
[2] K.N. Grew and W.K.S. Chiu. J. Power. Sources **199** (2012) 1.
[3] M.H. Zhao, Y. Xiang and J. Xu, Thin Solid Films **516** (2008) 7571.
[4] W.C. Oliver and G.M. Pharr, J. Mater. Res. **7** (1992) 1564.
[5] W.C. Oliver and G.M. Pharr, J. Mater. Res. **19** (2004) 3.
[6] M.W. Bai, K. Kato, N. Umehara and Y. Miyake, Thin Solid Films **377-378** (2000) 138.
[7] Y.C. Huang, S.Y. Chang and C.S. Chang, Thin Solid Films **517** (2009) 4857.
[8] J.R. Tuck, A.M. Korsunsky, S.J. Bull and R.I. Davidson, Surf. Coat. Technol. **137** (2001) 217.
[9] D. Beegan, S. Chowdhury and M.T. Laugier, Surf. Coat. Technol. **192** (2005) 57.
[10] M.T. Attaf, Mater. Lett. **57** (2003) 4627.
[11] M.T. Attaf, Mater. Lett. **58** (2004) 889.
[12] L. Zhou and Y.X. Yao, Mater. Sci. Eng. A **460-461** (2007) 95.
[13] X. Zhao, F. Wang, X. Wang and Z. Liu, J. Inorg. Mater. **26** (2011) 393.
[14] M.H. Zhao, X. Chen and Y. Xiang, Acta Mater. **55(18)** (2007) 6260.
[15] F.H. Wang and Y.L. Zhao, ICEM 2008: International Conference on Experimental Mechanics 2008, Proc. SPIE 7375, Nanjing, China, 2009.
[16] J. Johnson and J.M. Qu, J. Power. Sources **181** (2008) 85.
[17] A.J. Bushby, M.V. Swain, R.C. Bradt, C.A. Brooks and J.L. Roubort, Plastic Deformation of Ceramics, Plenum Press, New York, 1995 p. 231.
[18] M. Lichinchi, C. Lenardi, J. Haupt and R. Vitali, Thin Solid Films **312** (1998) 240.